Influence of the mechanical properties of nanoparticles on epoxy resin L

George PELIN*,[1], Cristina-Elisabeta PELIN[1]

*Corresponding author
[1]INCAS – National Institute for Aerospace Research "Elie Carafoli",
B-dul Iuliu Maniu 220, Bucharest 061126, Romania,
george.pelin@incas.ro*

DOI: 10.13111/2066-8201.2025.17.2.7

Received: 12 May 2025/ Accepted: 29 May 2025/ Published: June 2025

Abstract: *This paper presents an experimental study of the influence on the mechanical properties of L-type epoxy resin of three different types of nanometric powders (barium ferrite, Ni-doped carbon nanotubes and bismuth oxide, respectively) by obtaining three types of nanocomposites. Nanofillers are designed to modify the composition, to obtain materials adjustable to operating conditions by adapting their mechanical properties. The study consisted in dispersing a percentage of 1% by weight of each of the fillers in the epoxy resin. All samples were investigated from a mechanical point of view at room temperature environment, by tensile and 3-point bending tests. The failure mode and fractographic analysis were performed by optical microscopy.*

Key Words: *L-type epoxy resin, barium ferrite, CNT-Ni, bismuth oxide, mechanical properties, nanocomposites*

1. INTRODUCTION

The advantages that composite materials have brought to the aeronautical industry are very important because their low specific weight combined with high mechanical strength ensures significant reductions in vehicle mass and, implicitly, in fuel consumption and associated costs, and consequently increasing the safety of air transport.

The development and implementation of the fundamental technological concepts and systems for the development of intelligent structures is based on the development of intelligent composite structures, built up from constituent materials with a surface modified in various ways, in order to obtain materials resilient to the operating conditions by adapting mechanical, electromagnetic and other properties.

The novelty of the solutions lies in developing the concept of modifying conventional materials so that they behave similarly to smart materials, targeting various categories of properties.

Experimental studies aim to create new composite materials by incorporating compounds with electromagnetic properties into thermoresistant matrices and observing how they influence mechanical behavior [1].

In the literature it is observed that carbon-based nanomaterials (such as carbon nanotubes, graphene, reduced graphene oxide, etc.), conductive polymers (such as polypyrrole (PPy), polyaniline (PANI), etc.), metals and metal alloys, are preferred due to their reflective properties on EM waves, while ceramic nanoparticles (such as $BaTiO_3$, ZnO, Fe_3O_4, etc.) are preferred due to their EM wave absorption properties [2, 3]. The objectives in recent years have been to develop new absorbing/reflecting materials with improved characteristics, including low density, good thermal stability, broad absorption/reflection frequency, and oxidation resistance [2, 4, 5] along with increasing mechanical property values.

Bismuth oxide stood out through its versatile and environmentally friendly, non-hazardous compound, showed high efficiency in a wide range of fields such as catalysts, gas sensors, optical coatings, solar cells, antibacterial applications, antioxidants and enzyme inhibitors, due to their unique electrical, catalytic, magnetic and optical characteristics [6]. Bismuth oxide, due to its low weight, low cost and non-toxicity compared to pure lead, has been successfully used in recyclable polymers such as LDPE (low density polyethylene), LDPE/Bismuth Oxide nanocomposites [7].

C. V. Maestre and G. N. Santos [8] showed that the incorporation of Bi_2O_3 nanoparticles improves the protective efficacy of geopolymers, illustrating optimal results at different mass concentrations.

Ferrites have been widely used for electromagnetic applications, both Jan Kruzelak et al. [9] and M. H. Makled and T. Matsuiau [10] presented studies in which magnetic rubber composites were made by incorporating strontium ferrite and barium ferrite, respectively. The results indicated improved tensile mechanical properties for barium ferrite-based composites. Nanoscale barium ferrite ($BaFe_{12}O_{19}$) has been successfully used to obtain new polymer matrix composites (acrylic-butadiene-styrene (ABS)), as a filler applied by extrusion, and used in 3D printing [11]. For ethyl-cellulose-based nanocomposites, the successful use of barium ferrite magnetic nanopowder loading in the polymer matrix promised to significantly improve mechanical properties (tensile strength, elongation, and microhardness) compared to pure ethyl-cellulose [12].

Studies found in the literature show a real interest in using these nanometric agents to positively stimulate and improve the mechanical properties of both thermoplastic and thermosetting polymers.

The current study presents the use of three different compounds with known electromagnetic characteristics in epoxy matrix nanocomposites, illustrating a preliminary experimental phase focused on the evaluation of mechanical properties and fracture mode and how each of the three fillers influence them.

2. EXPERIMENTAL

2.1 Materials

The study involved obtaining nanocomposite materials based on thermosetting polymer with nanometric powder fillers, which are particularly recognized for their electromagnetic properties.

The thermosetting polymer used as the matrix was the epoxy resin L-diglycidyl ether of bisphenol A and hardener LT (previously known as EPH 161-3-aminomethyl-3,5,5-trimethylcyclohexylamine or isophoronediamine). The electromagnetic fillers consisted of 3 types of nanometric compounds, namely nickel-coated multiwalled carbon nanotubes (hereinafter referred to as MWCNT-Ni), nanometric Barium ferrite ($BaFe_{12}O_{19}$) and nanometric Bismuth oxide (Bi_2O_3). The properties of the materials used in the study are detailed in Table 1.

Table 1 – Materials used in the experimental study and their main characteristics

Material	Characteristics	Supplier
Epoxy Resin L	Name: Bisphenol A diglycidyl ether (DGEBA) Density: 1.14 g/cm3/23 °C Viscosity: 700 mPa*s/25 °C Epoxy value: 0.56 100/equivalent Epoxy equivalent: 179 g/equivalent Chloride content <1% Hydrolyzable chloride content < 500 ppm Vapour pressure <1 mbar/ 25 °C Refractive index: 1.547 nD25 Flash point (ISO 3679) > 150 °C Storage time (sealed, at 15 °C): 36 months	R&G Composites
LT Hardener (EPH161)	Name: Isophoronediamine (IPDA) Processing time 100 g mixture with L20: 90 min/ 20°C Mixing ratio per 100 g L20 mass fraction: 25 g Density: 1.0 g/cm2/20 °C Storage time (sealed, at 15 °C): 12 months	
Nickel-coated multi-walled carbon nanotubes (MWCNT-Ni)	Shape and color: black nanometric powder Outer diameter: 10-20nm Inner diameter: 5-10nm Length: 10-30um Ni content: >60wt% CNT content: >38wt% Specific surface area: 60 m2/g (by BET method) Production method: CVD (chemical vapour deposition)	Chengdu Organic Chemicals Co. Ltd.-Chinese Academy of Sciences
Barium Ferrite ($BaFe_{12}O_{19}$)	Form and color: brown nanometric powder Purity: >97% trace metals (Fe, Ba) based (by XRF) Particle size <100 nm (BET method) Molecular mass: 1111.46 g/mol	Sigma Aldrich (REDOX S.A)
Bismuth Oxide (Bi_2O_3)	Shape and color: yellow nanometric powder Bismuth content: >87.9% Purity: >99.8% Nanoparticle shape: spherical Nanoparticle size: 90-210 nm Specific surface area: 3.2-3.5 m2/g Density: 0.5 1.1 g/mL Molecular mass: 465.96 g/mol	

2.2 Obtaining method

All nanofilled samples were developed using the same method, which involves using ultrasonic homogenization to break up agglomeration zones and distribute them evenly throughout the resin mass. When the size of the particles size used is nanometric, the very high values of their specific surface area (surface area to volume ratio) determine a strong agglomeration phenomenon, which generates adhesion of nanoparticles to each other, thus leading to a polymer-nanopowder mixture with inhomogeneous composition. This inhomogeneous character generates extremely strong negative effects in terms of mechanical properties. By using ultrasonic mixing, instead of mechanical mixing, the propagation of high-intensity ultrasonic waves through the liquid phase, by creating local pressures and temperatures, determines the breakage of nanoparticle agglomerates and their uniform dispersion in the liquid [13], as illustrated in Fig. 1.

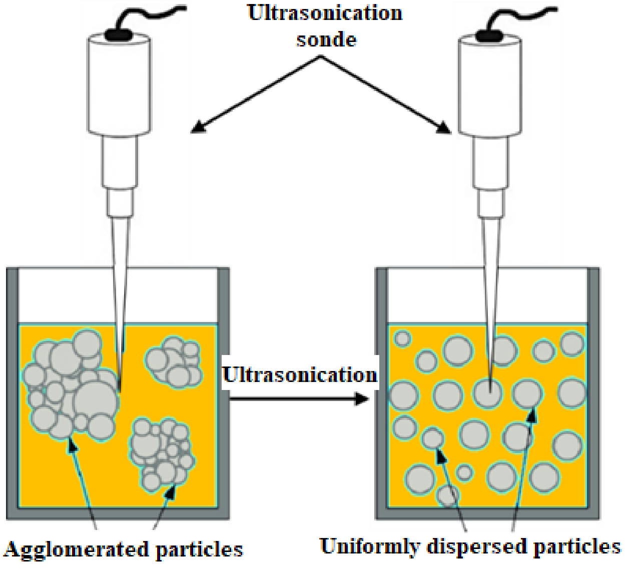

Fig. 1 – Dispersion of nanosized particles in polymeric fluids using ultrasound (adapted from [13])

The ultrasonication of the mixtures is done in 10 short cycles, of maximum 1 minute/burst. The temperature of the mixture is maintained constant throughout the sonication cycle, by immersing the glass in an ice bath, to avoid damaging the structure of the multilayer walls in the case of carbon nanotubes in particular.

The hardener is added after the ultrasonication step, by slow manual mixing, using a mixing rod for approximately 2-3 minutes, so that the homogeneity of the ultrasonicated mixture is as little affected as possible.

The mixture is then placed in Teflon molds with shapes and dimensions specific to mechanical tests (tensile and 3-point bending, respectively) and subjected to vacuum pressure (2 bars) for 24 hours, during which time the cross-linking reaction takes place completely.

Fig. 2 – The obtained nanocomposites: (a) Control Epoxy, (b) Epoxy+1%CNT-Ni, (c) Epoxy+1%$BaFe_{12}O_{19}$, (d) Epoxy+1%Bi_2O_3

2.3 Testing methods

The mechanical tests consisted of quasi-static 3-point tensile and bending tests, performed at room temperature, using the INSTRON 5982 equipment, equipped with a 10 kN force cell and an optical (video) extensometer (AVE) with a viewing field of 200 mm. Data acquisition and processing was performed using the dedicated Bluehill Universal software. Fractographic analysis was performed by optical microscopy using MEIJI ML8520 optical microscope, equipped with video camera for data acquisition. Images were captured at two magnification levels 40x and 200x.

3. RESULTS AND DISCUSSIONS

3.1 Mechanical tensile testing

Tensile testing was performed in accordance with the international standard ISO 527-1:2019 Plastics — Determination of tensile properties, with a test speed of 5 mm/min [14]. A number of 3-5 samples (fig. 3) were tested per nanocomposite type, and the averaged results are illustrated in Table 2 and Fig. 4.

Table 2 – Average values of tensile mechanical properties of nanocomposites

Materials	Load (kN)	Modulus (GPa)	Tensile stress (MPa)	Tensile strain (%)	Poisson's ratio (Chord)
Control Epoxy	1.57	3.31	45.08	1.49	0.58
Epoxy+1%Bi_2O_3	2.08	3.61	53.11 ↗	1.66	0.45
Epoxy+1%CNT-Ni	1.8	3.84	46.07 ↗	1.06	0.5
Epoxy+1%$BaFe_{12}O_{19}$	1.89	3.46	48.79 ↗	1.63	0.1

The average numerical values of the mechanical tensile results improve in the presence of all 3 nanometric compounds, compared to the results of the control sample made of type L epoxy resin. Significant increase in tensile strength, compared to the control sample, is presented by the sample with barium ferrite, approximately 17.8%, followed by the sample with Bi_2O_3, approximately 8.3%, and the sample with CNT-Ni shows an increase of approximately 2.2%.

Fig. 3 – Samples before and after tensile test: A- Control Epoxy; B- Epoxy+1%Bi_2O_3; C- Epoxy+1%CNT-Ni; D- Epoxy+1%$BaFe_{12}O_{19}$

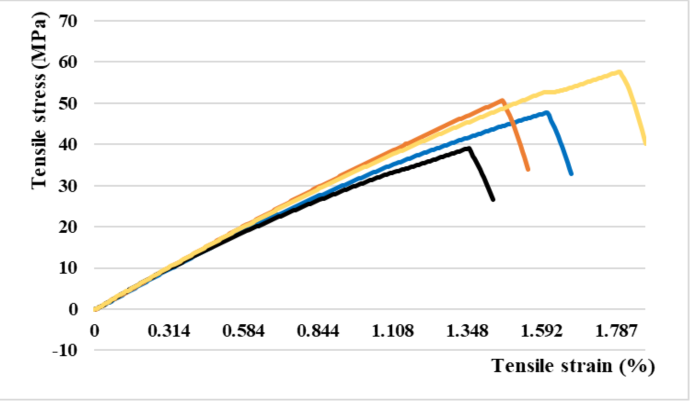

Fig. 4 – The resistance/elongation graph for the tensile testing of the obtained

The 3-point bending testing was performed in accordance with the international standard ISO 178:2019 Plastics — Determination of flexural properties, with a test speed of 2 mm/min [15]. A number of 3-5 samples (Fig. 5) were tested to failure for each type of nanocomposite, and the averaged results are illustrated in Table 3 and Fig. 6.

Table 3 – Average values of 3-point bending test properties of nanocomposites

Materials	Modulus (GPa)	Flexure stress (MPa)	Flexure strain (%)	Force (N)
Control Epoxy	3.65	79.02	2.16	150.24
Epoxy+1%Bi_2O_3	3.59	85.32 ↗	2.34	224.48
Epoxy+1%CNT-Ni	3.88	81.75 ↗	2.07	175.32
Epoxy+1%$BaFe_{12}O_{19}$	3.62	106.86 ↗	3.14	222.52

The averaged numerical values of the mechanical results at 3-point bending improve following in the presence of all 3 nanometric compounds compared to the values of showed by the control sample from type L epoxy resin. A significant increase for 3-point bending stress, compared to the control sample, is shown by the sample with the 1% barium ferrite, approximately 35%, followed by the sample with 1 % Bi_2O_3, approximately 8%, and the sample with CNT-Ni which shows increases of approximately 3.5%.

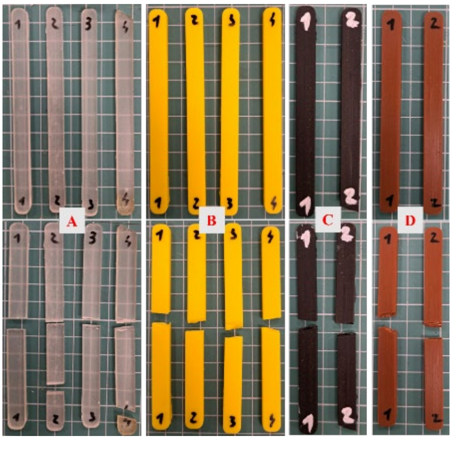

Fig. 5 – Samples before and after 3-point bending test: A- Control Epoxy; B- Epoxy+1%Bi_2O_3; C- Epoxy+1%CNT-Ni; D- Epoxy+1%$BaFe_{12}O_{19}$

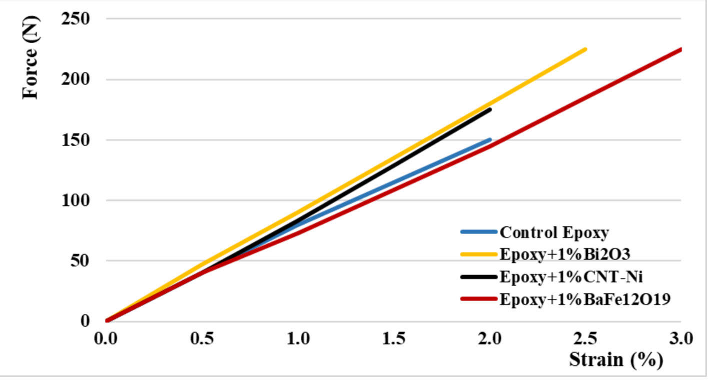

Fig. 6 – The 3-point bending strength-elongation graph of the obtained nanocomposites

3.2 Fractographic analysis

Fractographic analyses consisted of microscopic analyses, using optical microscope, at low magnification levels of 40x and 200x with the aim of identifying the fracture mode and the main mechanism that led to the sample failure following tensile testing.

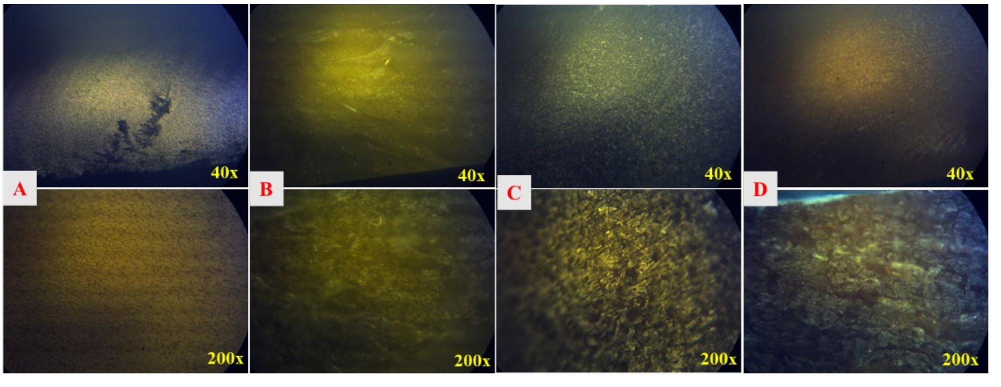

Fig. 7 – Optical microscopy images registered in the failure area with a 40x and 200x magnifications for: A- Control Epoxy; B- Epoxy+1%Bi_2O_3; C- Epoxy+1%CNT-Ni; D- Epoxy+1%$BaFe_{12}O_{19}$

Optical analysis highlights the failure mode that occurred during mechanical stress, but also the morphology of the material and the influence of the nanoparticles presence on the nanocomposite structure and mechanical behaviour.

All samples illustrate their brittle nature shown by the fracture mode. The images of the Control Epoxy, both at 40x and 200x magnification, illustrate glassy areas, with microcracks throughout the analyzed area.

For specimens with nanofillers, the optical images illustrate crystalline areas, with a rough appearance. No microcracks are observed at the levels ensured by optical microscopy investigation.

For further evaluation of the sample morpho-structure and homogeneity as well as nanoparticles distribution, next stage of the experimental study will involve the use of scanning electron microscopy that can provide suitable magnification levels that allow the visualisation of the nanoparticles embedded into the resin and can emphasize the differences when adding different particles as well as eventual agglomerated areas. The levels provided by optical microscopy indicate a compact morphology, without large size agglomerated areas or voids.

4. CONCLUSIONS

By adding nanofillers to polymers, new electromagnetic shielding materials with improved mechanical properties can be obtained, due to the synergistic effects of nanofillers and ferromagnetic compounds.

In this study, new composite materials with 1% by weight electromagnetic compounds were obtained and mechanically characterized by standard tests (tensile and bending at room temperature), in order to observe the influence of nanometric fillers on the mechanical properties. Type L epoxy resin was used as the polymer matrix. The nanopowders used were nickel-coated multiwall carbon nanotubes (MWCNT-Ni), nanometric Barium ferrite ($BaFe_{12}O_{19}$) and nanometric Bismuth oxide (Bi_2O_3). A percentage of 1% by mass of each nanometric powder was used, relative to the mass of the epoxy resin.

The mechanical characteristics improved when adding each of the three compounds, both the strength and the modulus of elasticity showed higher values compared to the results of the control sample. Barium ferrite generated the highest increments in all tested properties, followed by bismuth oxide and Ni-coated CNT. The next stages of the experimental study, currently under development will involve specific electromagnetic testing, thermal testing as well as morpho-structural characterization.

ACKNOWLEDGMENT

This work was supported by a grant of the Ministry of Research, Innovation and Digitization, Nucleu Program 36 N/12.01.2023/ Project PN 23 17 03 01/2023.

REFERENCES

[1] G. S. K. Sharma, Flying smart: Smart materials used in aviation industry, *Materials Today: Proceedings,* vol. **27**, no. 1, , pp. 244-250, 2020.

[2] Y. A. A. S. A. C. A. M. a. M. J. N. N. Ali, Comparative study of microwave absorption characteristics of (Polyaniline/NiZn ferrite) nanocomposites with different ferrite percentages, *Materials Chemistry and Physics,* vol. **211**, no. https://doi.org/10.1016/j.matchemphys.2018.02.017, pp. 79-87, 2018.

[3] K. J. V. P. C. R. G. M. P. J. Bora, Electromagnetic interference shielding efficiency of MnO2 nanorod doped polyaniline film, *Materials Research Express,* vol. **4**, no. no. 2, DOI 10.1088/2053-1591/aa59e3, p. 025013, 2017.

[4] Z. L. X. W. J. Z. S. H. Y. H. . Zhan, 3D carbon fiber mats/nano-Fe3O4 hybrid material with high electromagnetic shielding performance, *Applied Surface Science,* vol. **444**, no. https://doi.org/10.1016/j.apsusc.2018.03.006, pp. 710-720, 2018.

[5] X. W. W. C. C. H. H. Y. J. Y. M.-S. C. J. Ma, A facile fabrication and highly tunable microwave absorption of 3D flower-like Co3O4-rGO hybrid-architectures, *Chemical Engineering Journal,* vol. **339**, no. https://doi.org/10.1016/j.cej.2018.01.152, pp. 487-498, 2018.

[6] M. W. N. A. M. U. M. W.-U.-R. M. A. S. A.-O. S. S. Alam, Facile Green Synthesis of α-Bismuth Oxide Nanoparticles: Its Photocatalytic and Electrochemical Sensing of Glucose and Uric Acid in an Acidic Medium, *Journal of Composites Science,* vol. **8**, no. no. 2, https://doi.org/10.3390/jcs8020047, p. 47, 2024.

[7] S. M. A. E. A. M. A. A. A. S. A. Alshahri, LDPE/Bismuth Oxide Nanocomposite: Preparation, Characterization and Application in X-ray Shielding, *Polymers,* vol. **13**, no. no. 18, https://doi.org/10.3390/polym13183081, p. 3081, 2021.

[8] G. N. S. C. V. Maestre, Effect of bismuth oxide nanoparticle on the electromagnetic interference shielding and thermal stability of industrial waste based-geopolymer composites, *Sci Rep,* vol. **13**, no. https://doi.org/10.1038/s41598-023-27623-2, p. 1787, 2023.

[9] M. M. R. D. I. H. Jan Kruzelak, Barium and strontium ferrite-filled composites based on NBR and SBR, *Journal of Elastomers & Plastics,* vol. **51**, no. NO. 5, Doi:10.1177/0095244318792036, pp. 421-439, 2018.

[10] T. M. M. H. Makled, Magnetic and mechanical characterisation of natural rubber coprecipitated barium ferrite composites at high loading, *Plastics, Rubber and Composites,* vol. 38, no. NO. 7, https://doi.org/10.1179/146580109X12473409436706, pp. 297-301, 2009.

[11] D. S. D. N. Thomas Hanemann, 3D Printing of ABS Barium Ferrite Composites, *Materials,* vol. 13, no. NO.6, https://doi.org/10.3390/ma13061481, p. 1481, 2020.

[12] I. R. V. Ć. A. G. J. S.-T. R. J.-H. Aleksandar Stajčić, The Influence of Barium Ferrite Nanoparticles on Morphological and Mechanical Properties of Ethyl Cellulose Based Nanocomposites, *Science of Sintering,* vol. **51**, no. doi:https://doi.org/10.2298/SOS1903277S, pp. 277-283, 2019.

[13] S. Mahanta, M. Chandrasekaran, S. Samanta and C. Sasikumar, Fabrication of Al7075-B4C-fly ash hybrid nanocomposites by ultrasonic assisted stir casting and tensile analysis, *AIP Conf. Proc. ,* vol. 2128, no. https://doi.org/10.1063/1.5117938, p. 020026, 2019.

[14] * * * ISO 527-1 Plastics — Determination of tensile properties, 2019.

[15] * * * ISO 178 Plastics — Determination of flexural properties, 2019.